Journal of the Iranian Chemical Society (2022) 19:2739–2748
https://doi.org/10.1007/s13738-021-02487-3

ORIGINAL PAPER

Newly synthesized piperazine derivatives as tyrosinase inhibitors: in vitro and in silico studies

Cigdem Dokuzparmak[1] · Fulya Oz Tuncay[1] · Serap Basoglu Ozdemir[1] · Busra Kurnaz[1] · Ilke Demir[2] · Ahmet Colak[1] · Safiye Sag Erdem[2] · Nuri Yildirim[1]

Received: 9 May 2021 / Accepted: 27 December 2021 / Published online: 13 January 2022

Abstract

In this study, a series of new organic compounds with piperazine as a fundamental skeleton was synthesized and evaluated for their tyrosinase inhibitory potentials by in vitro and in silico studies. The in vitro studies have shown that compounds 10a and 10b bearing 1,2,4, triazole nucleus could be considered potent tyrosinase inhibitors with IC_{50} values of 31.2 ± 0.7 and 30.7 ± 0.2 μM, respectively. 10b ($K_i = 9.54$ μM, mixed type inhibition) with the lowest IC_{50} value among derivatives was selected to determine kinetic constants and inhibition types. Furthermore, molecular docking analysis was performed for all compounds and it was observed that 4b, 5a, 4c, and 10b showed promising inhibitory effect on tyrosinase activity. Based on docking results, ADME predictions and in vitro studies, 10b might be considered suitable oral drug candidates for further studies.

Keywords Tyrosinase inhibitor · Piperazine · Triazole · Molecular docking

Introduction

Tyrosinase, as a multifunctional enzyme containing binuclear copper, is widely found in animals, microorganisms and plants. It plays a crucial role in melanin biosynthesis since it catalyzes the conversion of monophenols and/or *o*-diphenols to suitable quinones, which then can be converted to melanins [1, 2]. Melanin, which is biosynthesized by tyrosinase throughout melanogenesis, is the main pigment found in animals' eyes, hair, and skin [3]. However, excessive melanin production or irregular distribution may cause albinism, skin cancer, irregular hyperpigmentation of the skin, such as melasma, freckles, and senile lentigo, and neurodegeneration, including Parkinson's diseases [4–6]. Melanin pigment reduction is not only used to prevent these disorders, but it is also used as a skin whitening agent for aesthetic concerns [7]. Hence, the interest in the melanogenesis modulation strategy is increasing gradually, considering the potential of rectifying problems associated with abnormal pigmentation in the skin [8, 9]. Moreover, one of the main issues that confront us caused by tyrosinase is a browning enzymatic reaction, which leads to rapid degradation of fruits and vegetables during the postharvest, storage, and handling processes [10, 11].

Widely considered a good way to handle all of these problems is regulating melanogenesis by inhibiting the tyrosinase activity. Therefore, tyrosinase inhibitors have found considerable interest in cosmetics, medicine, food, and agriculture. Over the last few decades, many tyrosinase inhibitors obtained from synthetic and natural origin have been investigated [7, 11, 12]. However, only a few can be used in some applications due to some side effects such as cytotoxicity and carcinogenicity [4, 7]. As a result, the requirement of designing novel and effective tyrosinase inhibitors is continually increasing. Therefore, many organic molecules are synthesized or isolated from natural products and investigated for their inhibitory effects on tyrosinase activity through in vitro and in silico application [13–16].

Heterocyclic compounds play a key role in new drug design and development. Therefore, they are accepted as a medically necessary class. Synthetic and medicinal chemists showed great interest in 1,2,4-triazole, 1,3,4-oxadiazole and 1,3-thiazole derivatives due to their different structures and regarded

✉ Ahmet Colak
acolak@ktu.edu.tr

[1] Department of Chemistry, Faculty of Science, Karadeniz Technical University, 61080 Trabzon, Turkey

[2] Department of Chemistry Faculty of Arts and Sciences, Marmara University, 34722 İstanbul, Turkey

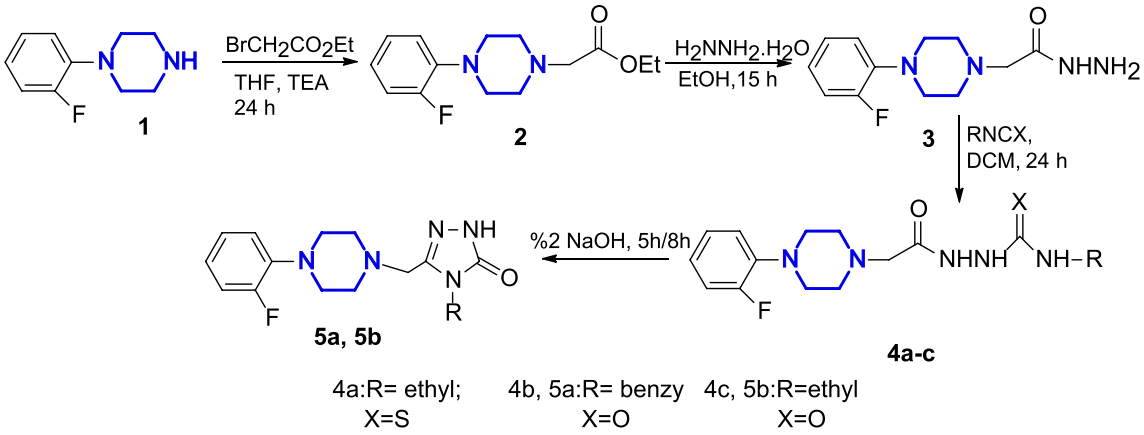

Scheme 1 Synthesis of compounds 2, 3, 4a-c, 5a, and 5b

them as useful tools for drug discovery processes [17–19]. One of the nitrogen-containing heterocycles, piperazine ring, has great importance in pharmaceutical and therapeutical fields [16] due to its effectiveness as anticancer [20], antimicrobial [21], antiviral agent [22], etc. Also, it is located in the structures of some vital drugs such as ciprofloxacin, levofloxacin [23], aplaviroc and imatinib [24].

The discovery of potential drug compounds is an expensive and time-consuming process. Computer-aided methods can be utilized in crucial rational drug design steps and cut down the cost considerably [25]. In addition to determine ADME properties of new drug candidate molecules for this purpose, molecular docking is one of the commonly used structure-based computer-aided drug design method that predicts binding affinity and conformations of small molecules (ligands) in the binding sites of target macromolecules (enzymes) [26].

In the present study, we aimed to synthesize some new piperazine derivative compounds and investigate them for their tyrosinase inhibitory potentials. For this purpose, in vitro tyrosinase inhibitory studies were carried out. The potential derivatives and inhibition type of the most effective one were defined. Additionally, to provide an insight into the inhibition mechanism, molecular docking of newly synthesized compounds was performed at the tyrosinase active site. Free energy of binding, the best binding orientation, and the respective intermolecular interactions were predicted for these compounds. ADME properties were determined as well to predict their bioavailability.

Results and discussion

Synthesis and characterization

In this study, the 2, 3, and 4a compounds were previously synthesized by us [27]. Reaction of the starting compound 1- (2-fluorophenyl) piperazine with ethyl bromo acetate gave Ethyl [4- (2-fluorophenyl) piperazin-1-yl] acetate (2). The structure of compound 2 was confirmed by the disappearance of broad singlet for NH and the presence of triplet at the 1.20 ppm and a quartet at 4.10 ppm due to ethyl group protons in the ^{1}H NMR spectrum. This group appeared at 14.6 ppm (CH_3) and 60.3 ppm (CH_2) in the ^{13}C NMR spectrum. The substitution of an ester group by hydrazide generated 2-[4-(2-Fluorophenyl)piperazine-1-yl]acetohydrazide (**3**), which were confirmed by the appearance of broad signal for -$NHNH_2$ group in FTIR spectrum. This group was recorded at 4.25 (NH_2) and 8.94 (NH) ppm in the ^{1}H NMR spectrum. The nucleophilic addition of compound **3** to alkyl(aryl)iso(thio) cyanates afforded the corresponding carbo(thio)amides (4a-4c). FTIR spectra of compounds 4a-4c revealed the presence of C = S group 1235 cm^{-1} for (4a), while C = O groups (for 4b, 4c) 1666 and 1661 cm^{-1}. Another evidence for the formation of carbo(thio)amides was three NH- signals at the range of 6.26–9.65 ppm in the ^{1}H NMR spectrum. Compounds 5a and 5b were obtained due to the cyclization of compounds 4b and 4c in the basic medium. The FTIR spectra of compounds 5a and 5b displayed -C = O stretching bands at 1701 and 1683 cm^{-1}. In the ^{1}H NMR spectra of compounds 5a and 5b**,** the NH signals were recorded at 11.77 and 11.54 ppm. In the ^{13}C NMR spectra, triazole C-3 and C-5 of compounds 5a and 5b resonated at 144.7 and 144.6 (triazole C-3), 155.9 and 155.5 (triazole C-5), respectively (Scheme 1).

The synthesis of compounds 10a and 10b was carried out by the treatment of NaOH in water under reflux condition, thereby introducing 1,2,4-triazole nucleus to piperazine skeleton. It is well known that bioactive compounds can be more effective if two or more biologically active heterocyclic systems are introduced to their structures as a single molecular framework [28–30] (Scheme 2). It is also known that 1,2,4-triazol-3-(thi)ol derivatives can be found in

mercapto-thioxo (or enol-keto) tautomeric forms. The –SH proton due to mercapto form resonates at about 13–14 ppm, while NH signal originated from thioxo tautomer appears at 9–12 ppm as D_2O exchangeable signals [28, 31]. These compounds exhibited FTIR, ^{1}H NMR, and ^{13}C NMR spectra consistent with the assigned structures. The –SH signal was recorded at 13.65 ppm in compound 10a. The NH signal of compound10b was recorded as 11.58 ppm. ^{13}C NMR spectra of these compounds have resonances of triazole C-3 and C-5 at 149.3–167.3 ppm and 144.5–155.6 ppm, respectively.

Tyrosinase inhibitory activity

The inhibition studies to reveal the inhibition potential of the synthesized compounds on the tyrosinase activity were carried out after the tyrosinase enzyme was optimized. Kojic acid was selected as the reference inhibitor molecule in this study. All findings obtained from these studies are presented in Table 1. As this table shows, IC_{50} values were determined only for eight compounds (4c, 5b, 7, 8, 9a, 9b, 10a, and 10b). The other five compounds (2, 3, 4a, 4b, and 5a) inhibited the tyrosinase by less than 25%. There are two possible explanations for this result. First, inhibitor molecules precipitated when we added their concentrated solutions to the reaction mixture containing a large amount of buffer solution. Therefore, the inhibitor concentration ranges are different for each compound. Second, the enzyme has been inhibited by less than 50% even if the compound's most concentrated stock solution is added to the reaction mixture. The one striking observation to emerge from the IC_{50} values in Table 1 was

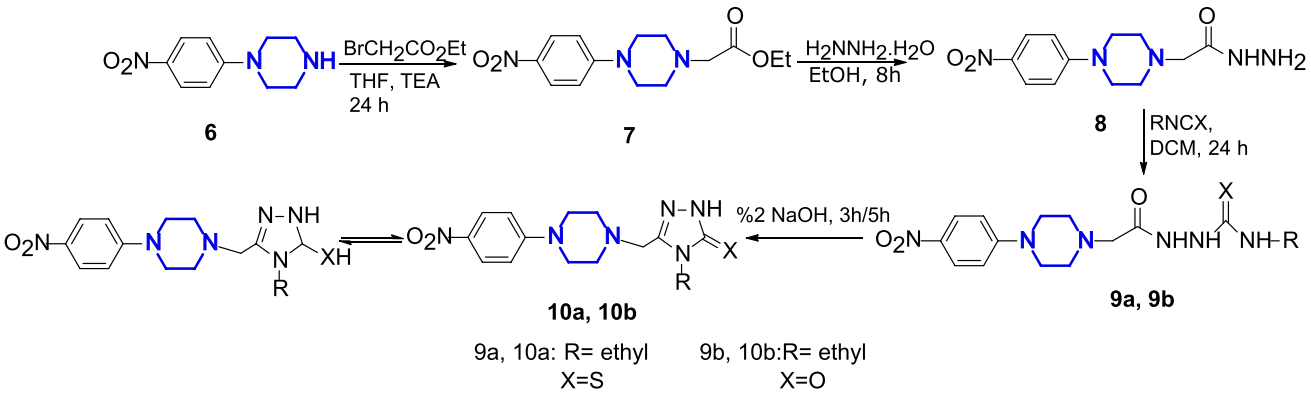

Scheme 2 Synthesis of compounds 7, 8, 9a, 9b, 10a, and 10b [34]

Table 1 Optimization values of tyrosinase activity, tyrosinase inhibitory effects and binding energies (ΔG) of newly synthesized compounds

Optimization values of tyrosinase activity		Inhibitor compounds	IC_{50}, μM	Max İnhibition		Binding Affinity (ΔG, kcal/mol)
				%	[I]*, μM	
		2	> 3000	23.7 ± 0.3	3000	− 6.4
		3	> 2900	17.0 ± 0.1	2900	− 7.2
		4a	> 100	5.1 ± 0.5	100	− 7.3
		4b	> 500	11.2 ± 0.2	500	− 8.6
		4c	651.3 ± 13.2	57.4 ± 1.3	1500	− 7.9
		5a	> 100	10.7 ± 1.0	100	− 8.0
		5b	738.2 ± 18.6	66.8 ± 1.8	1100	− 7.3
		7	196.4 ± 1.1	75.1 ± 0.8	750	− 6.5
		8	94.0 ± 0.9	86.6 ± 0.8	750	− 6.5
		9a	43.1 ± 0.9	85.8 ± 0.9	350	− 6.8
pH	5.0	9b	110.6 ± 0.8	82.4 ± 0.6	500	− 7.3
Temperature	25 °C	10a	31.2 ± 0.7	70.5 ± 1.3	200	− 6.6
Final tyrosinase conc	30 μg/mL	10b	30.7 ± 0.2	72.8 ± 0.5	120	− 7.4
K_m	0.17 mM	Kojic acid	14.3 ± 0.1	98.5 ± 0.1	100	

*Concentration of inhibitor compounds

that compounds 7, 8, 9a, 9b, 10a and 10b exhibited better inhibitory potential than compounds 4c and 5b. A possible explanation for these results may be the lack of nitro groups linked to phenyl rings in compounds 4c and 5b. Previously published studies have noted the importance of containing a nitro group at the phenyl ring's para position. This group can lead to an increase in the inhibitory potency [13, 15]. Additionally, the compounds 10a and 10b with IC_{50} values 31.2 ± 0.7 and 30.7 ± 0.2, respectively, showed the highest inhibitory effect among them. It seems possible that this result may be due to the presence of triazole substituents in their structures. This is consistent with what has been observed in previous studies, which examined the inhibitory effect of triazole derivatives on tyrosinase activity [32, 33]. In parallel to these data, our docking results confirm the importance of the nitro and triazole moieties as pharmacophore groups as explained in Section Molecular docking calculation.

Kinetic analysis

To extend our knowledge of compounds inhibition mechanisms, some kinetic analyses were performed in the presence of the most potent inhibitor compound. All synthesized compounds in this study derived from the same core (piperazine). It is well known that the molecules having the same core and similar skeleton tend to exhibit similar inhibition profile. Then, the compound with the smallest IC_{50} was selected (compound 10b) in terms of representing the compound group to investigate its inhibition mechanism and K_i value. The plot of 1/V versus 1/[S] in the presence of different concentrations of compound 10b gave a series of straight lines as shown in Fig. 1. If the concentrations of the compound 10b were increased in the reaction mixture, as can be seen from Table 2, K_m values increased while V_{max} values decreased. As shown in Fig. 1, compound 10b bound to both a free enzyme and enzyme–substrate complex and exhibited a mixed type inhibition toward tyrosinase enzyme [32]. The K_i value was determined as 9.54 µM.

ADME properties

ADME properties of all molecules evaluated for their tyrosinase inhibition potential in this study are given in Table 3. ADME properties of compounds 4c and 5b were calculated but of other compounds were extracted from the literature [34]. Drug-likeness is evaluated based on Lipinski's Rule of Five. According to this rule, molecular weight should be ≤ 500 Da, LogP should be ≤ 5 (or MLogP ≤ 4.15), the number of hydrogen bond acceptors should be ≤ 10 and the number of hydrogen bond donors should be ≤ 5 [35]. Calculated properties show that none of the compounds violate these four parameters. Besides, all compounds have fewer

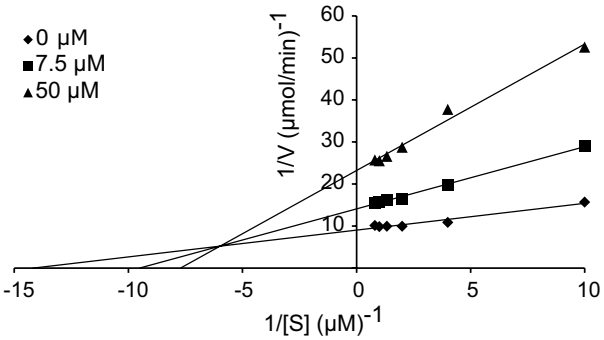

Fig. 1 Lineweaver–Burk plot for inhibition of tyrosinase in the presence of compound 10b

Table 2 Some kinetic parameters and type of tyrosinase inhibition in the presence of compound 10b

[Inhibitor] (µM)	K_m (mM)	V_{max} (µmol/dk.)	Inhibition type	K_i (µM)
0	0.07	0.11	Mix type	9.54
7.5	0.11	0.07		
50	0.13	0.04		

than ten rotatable bonds and less than 140 A^2 topological polar surface areas, confirming their good oral bioavailability [36]. Compounds show good percent absorption range from 66.73 to 97.69% as well.

Molecular docking calculation

According to the docking results, all compounds bind to the active site of the tyrosinase enzyme. The binding energies calculated for the piperazine derivatives range from −6.4 to −8.6 kcal/mol. The binding energies of the conformations that bind to the enzyme's active site with the lowest energy are given in Table 1.

As reported by in vitro inhibition studies, the five compounds showing high tyrosinase inhibition activity are 10b, 10a, 9a, 8 and 9b, respectively. The possible enzyme-inhibitor interactions that enable these compounds to show high inhibition activity were visualized. The amino acid residues and interactions that play critical roles in binding are presented in detail in Fig. 2 and Table 4.

Among the 13 compounds, 4b and 5a bind to the active site of tyrosinase with the highest binding affinities ($\Delta G \leq -8.0$) and, 4c, 10b, 5b, 9b and 4a are more potent inhibitors than other compounds ($\Delta G < -7.0$) (Table 1). This indicates that the results of the in silico studies are partially in agreement with in vitro studies. So, compound 10b is one of the top four molecules with highest binding affinity and binds to the enzyme efficiently as a strong inhibitor

Table 3 ADME properties of the newly synthesized piperazine compounds

Compound	%ABS	TPSA (A^2)	*n*-ROTB	MV	MW ≤ 500	LogP ≤ 5	*n*-ON ≤ 10	*n*-OHNH ≤ 5	*n*-Violation ≤ 1
2	97.69	32.78	5	249.04	266.32	2.29	4	0	0
3	87.75	61.60	3	230.38	252.29	−0.30	5	3	0
4a	88.43	59.63	7	305.12	339.44	1.48	6	3	0
4b	82.54	76.70	6	351.09	385.44	1.96	7	3	0
4c	82.54	76.70	5	296.25	323.37	0.94	7	3	0
5a	89.28	57.16	5	332.51	367.43	2.31	6	1	0
5b	89.28	57.16	4	277.66	305.36	1.09	6	1	0
7	81.88	78.61	6	267.44	293.32	2.13	7	0	0
8	71.94	107.42	4	248.79	279.30	−0.45	8	3	0
9a	72.62	105.45	8	323.53	366.45	1.32	9	3	0
9b	66.73	122.52	6	314.65	350.38	0.78	10	3	0
10a	80.36	83.02	5	305.60	348.43	2.01	8	0	0
10b	73.47	102.99	5	296.06	332.36	0.94	9	1	0

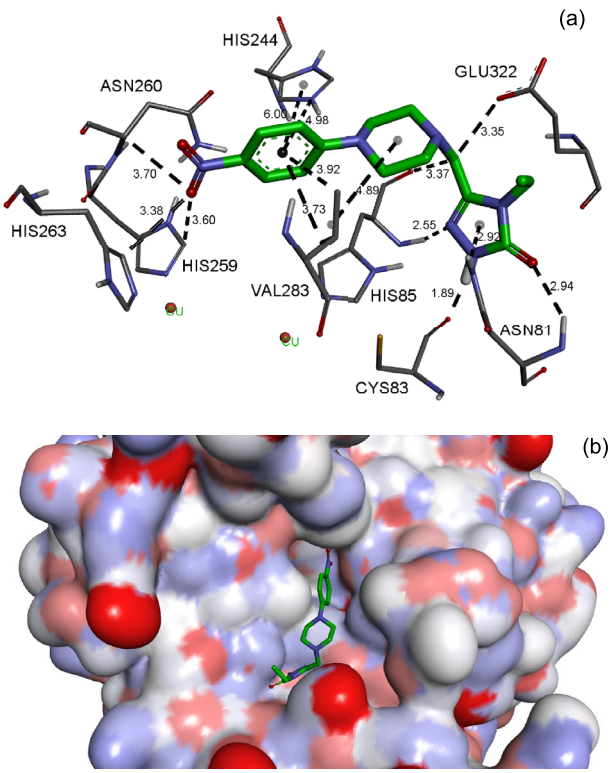

Fig. 2 Binding mode of compound 10b in the active site of tyrosinase enzyme. Interaction distances are given in A°. **(a)** micro-environment, **(b)** general projection

among the examined molecules (Table 1). As known, the results of docking and biochemical kinetic studies may not coincide completely. In addition, since docking methodology simulates a competitive inhibition, inhibitor molecules were interacted with target proteins in its active site when performing docking studies. On the other hand, bio-chemical kinetic studies showed that molecule 10b inhibited tyrosinase via mix inhibition mechanism which restrain the direct comparison of the binding affinities obtained from in silico and in vitro results. Nevertheless, docking is a powerful tool to predict the binding mode and pharmacodynamic interactions of the potent ligand molecules. For example, *p*-nitro phenyl group, piperazine and triazole rings in the structure of 10b are pharmacophore groups. These groups exhibit the following interactions for good binding: Carbon-H bonds between p-nitro group and His263, His259, Asn260; pi-donor and H-bond interactions between triazole ring and Asn81, hydrophobic interactions with the phenyl and piperazine rings, and His244, Val283.

Tyrosinase is an enzyme that contains two copper ions in its active site, and each copper is coordinated by three histidine residues, which are His259, His263, His296 and His61, His94, His85 in the X-ray structure (2Y9X) [37, 38]. According to the interactions occurred in enzyme active site, as seen in Table 4, compounds, 4c, 5b, 9b and 10b showed similar interactions with copper coordinated histidine residues. While 9b and 10b exhibit π-interactions and H-bond with His263, 4c and 5b interact with His85. Compound 10b also exhibits H-bonding interactions with His85 and His259. His244 located in the tyrosinase enzyme's active site but not coordinating with copper atoms and Glu322 located near the active site, interact with all four compounds. It is known that free histidine in the active site plays a vital role in enzyme activity [39]. Besides, Val283 and Asn260 show similar interactions with the majority of the compounds as well. Thus, these residues play essential roles in the tyrosinase inhibition mechanism. It appears that strong hydrogen bonds and hydrophobic interactions are mostly responsible for binding.

Table 4 Interactions of compounds 4c, 5b, 7, 8, 9a, 9b, 10a and 10b in the active site of the tyrosinase enzyme

Compound ID	ΔG (kcal/mol)	Residue	Interaction Type	Interaction Distance (A°)
4c	− 7.9	Glu322(O)…Ligand4c-NH(H)	H-Bond	2.81
		His85-C = O(O)…Ligand4c -NH(H)	H-Bond	2.75
		His85-C = O(O)…Ligand4c -NH(H)	H-Bond	2.12
		His85(C)…Ligand4c (F)	Carbon H-Bond	3.76
		Val283(C)…Ligand4c(piperazine ring)	Alkyl	4.67
		Val283(C)…Ligand4c(phenyl ring)	Pi-Sigma	3.92
		Asn260-NH_2(H)…Ligand4c(N)	H-Bond	2.75
		His244…Ligand4c(piperazine ring)	Pi-Alkyl	5.16
		Gly245-C = O(O)…Ligand4c(C)	Carbon H-Bond	3.74
5b	− 7.3	Val283(C)…Ligand5b(piperazine ring)	Alkyl	4.74
		Val283(C)…Ligand5b (C)	Alkyl	3.55
		Val283(C)…Ligand5b (phenyl ring)	Pi-Sigma	3.92
		His85-C = O(O)…Ligand5b -NH(H)	H-Bond	2.70
		His85…Ligand5b (C)	Pi-Alkyl	4.39
		Glu322(O)…Ligand5b -NH(H)	H-Bond	2.46
		His244…Ligand5b (piperazine ring)	Pi-Alkyl	5.12
7	− 6.5	His253(C)…Ligand7-NO_2(O)	Carbon H-Bond	3.79
		His263(C)…Ligand7-NO_2(O)	Carbon H-Bond	3.38
		Asn260(C)…Ligand30-NO_2(O)	Carbon H-Bond	3.53
		Val283(C)…Ligand7(phenyl ring)	Pi-Sigma	3.98
		Val283(C)…Ligand7(phenyl ring)	Pi-Sigma	3.75
		Val283(C)…Ligand7(piperazine ring)	Alkyl	5.11
		Asn81-NH_2(H)…Ligand7(O)	H-Bond	2.14
		His85-NH(H)…Ligand7-C = O(O)	H-Bond	2.28
		His85-C = O(O)…Ligand7(C)	Carbon H-Bond	3.74
		His85-C = O(O)…Ligand7(C)	Carbon H-Bond	3.66
8	− 6.5	Glu322(O)…Ligand8(C)	Carbon H-Bond	3.77
		Glu322(O)…Ligand8-NH(N)	Attractive charge	3.23
		Glu322(O)…Ligand8-NH_2(N)	Attractive charge	3.14
		Ala246-C = O(O)…Ligand8-NH_2(H)	H-Bond	2.57
		His244(C)…Ligand8-C = O(O)	Carbon H-Bond	3.48
		His244…Ligand8(piperazine ring)	Pi-Alkyl	4.97
		Asn260-NH_2(H)…Ligand8(phenyl ring)	Pi-donor H-Bond	3.02
		His259(C)…Ligand8-NO_2(O)	Carbon H-Bond	3.67
		Val283(C)…Ligand8(phenyl ring)	Pi-Sigma	3.87
9a	− 6.8	Phe264…Ligand9a(S)	Pi-Sulfur	5.27
		Asn260-NH_2(H)…Ligand9a -C = O(O)	H-Bond	2.12
		Asn260-C = O(O)…Ligand9a -NH(H)	H-Bond	2.52
		His85-C = O(O)…Ligand9a (C)	Carbon H-Bond	3.63
		Glu322(O)…Ligand9a (phenyl ring)	Pi-Anion	4.93
		Asn81-NH_2(H)…Ligand9a—NO_2(O)	H-Bond	2.97
		Asn81-NH(H)…Ligand9a—NO_2(O)	H-Bond	2.27
		Val283(C)…Ligand9a (piperazine ring)	Alkyl	5.14
		Gly281-C = O(O)…Ligand9a -NH(H)	H-Bond	2.43
		His263…Ligand9a (C)	Pi-Sigma	3.82

Table 4 (continued)

Compound ID	ΔG (kcal/mol)	Residue	Interaction Type	Interaction Distance (A°)
9b	− 7.3	His263…Ligand9b (C)	Pi-Sigma	3.76
		Asn260-C = O(O)…Ligand9b -NH(H) Asn260-	H-Bond	2.68
		C = O(O)…Ligand9b -NH(H)	H-Bond	2.90
		Asn260-NH_2(H)…Ligand9b -C = O(O)	H-bond	2.39
		His244-NH(H)…Ligand9b -C = O(O)	H-Bond	2.50
		Glu322(O)…Ligand9b (phenyl ring)	Pi-Anion	4.48
		Asn81-NH_2(H)…Ligand9b -NO_2(O)	H-Bond	3.00
		Asn81-NH(H)…Ligand9b -NO_2(O)	H-Bond	2.31
10a	− 6.6	His244…Ligand10a(triazole ring)	Pi-Pi T-shaped	4.92
		His244-NH(N)…Ligand10a (triazole ring)	Pi-Cation	4.47
		His244…Ligand10a -SH(S)	Pi-Sulfur	4.89
		Glu322(O)…Ligand10a -SH(H)	H-Bond	2.47
		Val248(C)…Ligand10a (triazole ring)	Pi-Alkyl	4.28
		Val248(C)…Ligand10a (piperazine ring)	Alkyl	4.94
		Val283(C)…Ligand10a (phenyl ring)	Pi-Sigma	3.52
10b	− 7.4	His263(C)…Ligand10b -NO_2(O)	Carbon H-Bond	3.38
		His259(C)…Ligand10b -NO_2(O)	Carbon H-Bond	3.60
		Asn260(C)…Ligand10b -NO_2(O)	Carbon H-Bond	3.70
		His244…Ligand10b (phenyl ring)	Pi-Pi T-shaped	6.00
		His244-NH(N)…Ligand10b (phenyl ring)	Pi-Cation	4.98
		Val283(C)…Ligand10b (phenyl ring)	Pi-Sigma	3.73
		Val283(C)…Ligand10b (phenyl ring)	Pi-Sigma	3.92
		Val283(C)…Ligand10b (piperazine ring)	Alkyl	4.89
		Glu322(O)…Ligand10b (C)	Carbon H-Bond	3.35
		His85-C = O(O)…Ligand10b (C)	Carbon H-Bond	3.37
		His85-NH(H)…Ligand10b (N)	H-Bond	2.55
		Cys83-C = O(O)…Ligand10b -NH(H)	H-Bond	1.89
		Asn81-NH_2(H)…Ligand10b (triazole ring)	Pi-donor H-Bond	2.92
		Asn81-NH(H)…Ligand10b -C = O(O)	H-Bond	2.94

Conclusions

In summary, the present study was designed to determine the inhibitory effect of some newly synthesized piperazine derivatives on tyrosinase activity. Among all the derivatives, compounds 10a and 10b bearing with respective triazole-3-thiol and triazole-3-one moieties (IC_{50} values 31.2 ± 0.7 and 30.7 ± 0.2, respectively) showed a promising effect on anti-tyrosinase activity. The molecular docking studies showed that compounds 10b, 4c, 4b, and 5a have higher potentials to be a tyrosinase inhibitor. Consequently, when the in vitro inhibition and docking results are evaluated together, in the view of good ADME properties, the evidence from this study suggests that compound 10b might be used as an oral drug candidate with a high potency in the pharmaceutical field for further studies.

Materials and methods

General

All reagents and solvents were purchased from Merck, Fluka, and Sigma Aldrich and used without further purification. Reactions were monitored by thin-layer chromatography (TLC) on silica gel 60 F254 aluminum sheets. Melting points of the synthesized compounds were determined in open capillaries on a Büchi B-540 melting point apparatus and are uncorrected. FTIR spectra were recorded using a Perkin Elmer 1600 series FTIR spectrometer. ^{1}H NMR and ^{13}C NMR spectra were registered in DMSO-d_6 on a BRUKER AVANCE II 400 MHz NMR spectrometer (400.13 MHz for ^{1}H and 100.62 MHz for ^{13}C). The mass

spectra were obtained on a Thermo TSQ Quantum Access Max Quattro Instrument.

Synthesis

The compounds 2, 3, 4a-b, 5a, 7, 8, 9a-b, and 10a-b were synthesized and studied for their potential to be inhibitors of amylase, previously by our research group [34]. In this study, compounds 4c and 5b were newly synthesized and all compounds were evaluated in terms of their tyrosinase inhibitory potentials for the first time.

General procedure for the synthesis of compounds 4c

The compound of **3** (10 mmol) and ethyl isocyanate (20 mmol) in dichloromethane was stirred at room temperature for 24 h. After evaporating the solvent under reduced pressure, a solid is obtained. The crude product was crystallized appropriate solvent.

4.4. *N*-ethyl-2-{[4-(2-fluorophenyl)piperazine-1-yl] acetyl}hydrazinecarboxamide (4c)

This crude product was crystallized from dimethylformamide: water (1:3). Yield: 86%, m.p: 150–151 °C. FTIR (ν_{max}, cm^{-1}): 3273 (NH), 3089 (Aromatic CH), 2977 (Aliphatic CH), 1661 (2C = O).^{1}H NMR (DMSO-d_6, δ ppm): 0.97 (t, 3H, CH_3, J = 6.8 Hz), 2.62 (s, 4H, $2CH_2$), 2.98–3.05 (m, 8H, $4CH_2$), 6.26 (s, 1H, NH), 7.00–7.09 (m, 4H, ArH), 7.67 (s, 1H, NH), 9.33 (s, 1H, NH).^{13}C NMR (DMSO-d_6, δ ppm): 15.9 (CH_3), 34.5 (CH_2), 50.4 (CH_2), 50.4 (CH_2), 53.2 ($2CH_2$), 60.1 (CH_2), arC: [116.3 (d, CH, $J_{C\text{-}F}$ = 20.0 Hz), 119.6 (d, CH, $J_{C\text{-}F}$ = 3.0 Hz), 122.6 (d, CH, $J_{C\text{-}F}$ = 8.0 Hz), 125.2 (d, CH, $J_{C\text{-}F}$ = 4.0 Hz), 140.3 (d, C, $J_{C\text{-}F}$ = 8.0 Hz), 155.4 (d, C, $J_{C\text{-}F}$ = 283.0 Hz)], 158.3 (C = O), 169.4 (C = O). LC MS/MS *m/z* (%): 346.13 ($[M+Na]^+$, 100), 324.15 ($[M+1]^+$, 38).

General procedure for the synthesis of compounds 5b

A solution of the corresponding compound 4 (10 mmol) is refluxed in the presence of a 2% NaOH solution for 4 h for 5b. Then, the solution was cooled to room temperature and its pH adjusted to 7.0 by adding 37% HCl. The precipitate formed was filtered and washed with water. This compound was recrystallized from the appropriate solvent.

4.6. 4-Ethyl-5-{[4-(2-fluorophenyl)piperazine-1-yl] methyl}-2,4-dihydro-3*H*-1,2,4-triazole-3-one (5b)

This crude product was crystallized from dimethyl sulfoxide: water (1:3). Yield: 70%, m.p: 216–218 °C. FTIR (ν_{max}, cm^{-1}): 3178 (NH), 3089 (Aromatic CH), 2988 (Aliphatic CH), 1683 (C = O). ^{1}H NMR (DMSO-d_6, δ ppm): 1.18 (t, 3H, CH_3, J = 7.2 Hz), 2.47–2.49 (m, 4H, $2CH_2$), 2.97 (s, 4H, $2CH_2$), 3.43 (s, 2H, CH_2), 3.64 (q, 2H, CH_2, J = 7.2 Hz), 6.92–7.11 (m, 4H, ArH), 11.54 (s, 1H, NH). ^{13}C NMR (DMSO-d_6, δ ppm): 14.6 (CH_3), 36.1 ($2CH_2$), 50.5 (CH_2), 52.9 ($2CH_2$), 53.3 (CH_2), arC:[116.1 (d, CH, $J_{C\text{-}F}$ = 26.0 Hz), 119.7 (CH), 122.8 (d, CH, $J_{C\text{-}F}$ = 16.0 Hz), 125.2 (CH), 140.1 (d, C, $J_{C\text{-}F}$ = 9.0 Hz), 155.4 (d, C, $J_{C\text{-}F}$ = 243.0 Hz)], 144.6 (triazole C-3), 155.5 (triazole C-5). LC MS/MS *m/z* (%): 328.28 ($[M+Na]^+$, 100), 306.23 ($[M+1]^+$, 67).

Tyrosinase assay and activity optimization

Tyrosinase activity was investigated as stated in a previous method with slight modifications by using *L*-tyrosine as a substrate [40]. In detail, 979 µL citrate–phosphate buffer solution (50 mM, pH 5.0), 120 µL MBTH solution (10 mM), 24 µL DMF, and 41 µL *L*-tyrosine solution (5 mM) were mixed in an Eppendorf tube and transferred to a spectrophotometer cuvette. After the enzyme addition into the reaction mixture, the absorbance immediately was read for 3 min at 475 nm. Before inhibition studies, the enzyme optimization studies (determination of optimum pH, optimum temperature, optimum protein concentration, and K_m value) were performed separately [41]. One enzyme activity unit was given as 1 µmol of product released in 1 min under reaction conditions [42].

Inhibition studies

Stock solutions of the synthesized compounds (as inhibitor) and kojic acid (positive control) were prepared in DMSO. The enzyme (36 µL) and inhibitor solution (12µL) were mixed and pre-incubated at room temperature for 10 min. Subsequently, substrate solution and other components were added into each reaction mixture, and absorbance measurements were performed. IC_{50} values of each inhibitor molecule were calculated from the relative activities (%)-inhibitor concentrations plot. All experiments were performed in triplicate.

Determination of inhibition type and kinetic constants

The compound with the smallest IC_{50} value (10b) was selected to determine its kinetic constants and inhibition type. The activity studies were carried out in the range of 0.25–5 km substrate concentration and in the absence and presence two different concentrations (causing 25–75% inhibition) of these inhibitors. Lineweaver–Burk plot was prepared using the data obtained from here, and the kinetic values and inhibition type were estimated.

Determination of ADME properties

While ADME properties of 11 compounds were calculated before [34], ADME properties of compounds 4c and 5b were estimated newly by using Molinspiration web server [43]. Physicochemical parameters such as percentage absorption (% ABS), topological polar surface area (TPSA), number of rotatable bonds (n-ROTB), molecular volume (MV), molecular weight (MW), the logarithm of n-octanol/water partition coefficient (miLog P), number of hydrogen bond acceptors (n-ON) and number of hydrogen bonds donors (n-OHNH) were calculated. Percentage absorption (%ABS) was calculated using TPSA with the following equation: %ABS = 109-(0.345xTPSA) [44].

Ligand preparation and molecular docking

3-D structures of 13 compounds were prepared using Spartan16 software [45]. Conformer search was applied to each compound with molecular mechanics/MMFF method. 50 conformations with the lowest energy were selected and optimized with the semi-empirical PM6 process [46]. Geometry optimizations of the most stable conformations were then performed with DFT/M06-2X/6-31G** method [47, 48] and used as ligands for docking calculations. They were docked into the active site of the X-ray crystal structure of *Agaricus bisporus* mushroom tyrosinase enzyme (PDB ID: 2Y9X, resolution 2.78 A°, co-crystalized with tropolone) [37]. AutoDock Vina and AutoDock Tools software were employed for all docking calculations [49, 50]. The amino acid residues Glu256, Asn260, Met280, Phe264, Val 283, and Ser282 in the enzyme's active site, and the ligand were selected as flexible. A grid box size of $40 \times 40 \times 40$ points in x, y, and z directions were built in the enzyme's active site. Water molecules, holmium atoms, B, C, D, F, G, H chains and tropolone inhibitor were removed from the X-ray structure, and hydrogen atoms were added. For validation of the docking protocol, the tropolone inhibitor in the X-ray structure was removed and re-docked to the enzyme. RMSD value was found to be $0.457 > 2$ to validate our protocol. For each compound, docking calculations were repeated ten times, and 90 conformations were obtained. The best docking pose with the highest binding affinity was chosen. The enzyme-ligand interactions were examined using Discovery Studio 4.5 Client software [51].

Supplementary Information The online version contains supplementary material available at https://doi.org/10.1007/s13738-021-02487-3.

Acknowledgements This work was supported by the Scientific and Research Council of Turkey (TUBITAK) [No. 117Z199].

Funding This work was supported by the Scientific and Research Council of Turkey (TUBITAK) [No. 117Z199], which is hereby gratefully acknowledged.

Declarations

Conflicts of interest The authors report no conflict of interest.

References

1. C.S. Nunes, K. Vogel, in Enzymes, in *Human and Animal Nutrition*. ed. by C.S. Nunes, V. Kumar (Elsevier, Academic Press, 2018), pp. 403–412
2. Á. Sánchez-Ferrer, J. Neptuno Rodríguez-López, F. García-Cánovas, F. García-Carmona, *Biochim. Biophys. Acta*, **1247**(1), 1–11 (1995). https://doi.org/10.1016/0167-4838(94)00204-T
3. G. Prota, Med. Res. Rev. **8**(4), 525–556 (1988). https://doi.org/10.1002/med.2610080405
4. H. Ando, H. Kondoh, M. Ichihashi, V.J. Hearing, J. Invest. Dermatol. **127**(4), 751–761 (2007). https://doi.org/10.1038/sj.jid.5700683
5. L.L. Baxter, W.J. Pavan, Wiley Interdiscip. Rev. Dev. Biol. **2**(3), 379–392 (2013). https://doi.org/10.1002/wdev.72
6. T. Hasegawa, Int. J. Mol. Sci. **11**(3), 1082–1089 (2010). https://doi.org/10.3390/ijms11031082
7. T. Pillaiyar, M. Manickam, V. Namasivayam, J. Enzyme Inhib. Med. Chem. **32**(1), 403–425 (2017). https://doi.org/10.1080/14756366.2016.1256882
8. S. Briganti, E. Camera, M. Picardo, Pigment Cell Res. **16**(2), 101–110 (2003). https://doi.org/10.1034/j.1600-0749.2003.00029.x
9. L. Ni-Komatsu, C. Tong, G. Chen, N. Brindzei, S.J. Orlow, Mol. Pharmacol. **74**(6), 1576–1586 (2008). https://doi.org/10.1124/mol.108.050633
10. R.F. Hurrell, P.-A. Finot, Adv. Exp. Med. Biol. **177**, 423–435 (1984). https://doi.org/10.1007/978-1-4684-4790-3_20
11. M.R. Loizzo, R. Tundis, F. Menichini, Compr. Rev. Food Sci. F. **11**(4), 378–398 (2012). https://doi.org/10.1111/j.1541-4337.2012.00191.x
12. S. Parvez, M. Kang, H.-S. Chung, H. Bae, Phytother. Res. **21**(9), 805–816 (2007). https://doi.org/10.1002/ptr.2184
13. T. Damghani, S. Hadaegh, M. Khoshneviszadeh, S. Pirhadi, R. Sabet, M. Khoshneviszadeh, N. Edraki, J. Mol. Struct. **1222**, 128876–128876 (2020). https://doi.org/10.1016/j.molstruc.2020.128876
14. D. Yang, L. Wang, J. Zhai, N. Han, Z. Liu, S. Li, J. Yin, Food Chem. **336**, 127714–127714 (2021). https://doi.org/10.1016/j.foodchem.2020.127714
15. H. Hosseinpoor, A. Iraji, N. Edraki, S. Pirhadi, M. Attarroshan, M. Khoshneviszadeh, M. Khoshneviszadeh, Chem. Biodivers. **17**(8), e2000285 (2020). https://doi.org/10.1002/cbdv.202000285
16. H. Raza, M. A. Abbasi, R. Aziz ur, S. Z. Siddiqui, M. Hassan, Q. Abbas, H. Hong, S. A. A. Shah, M. Shahid, S. Y. Seo, *Bioorg. Chem.*, **94**, 103445–103445 (2020). https://doi.org/10.1016/j.bioorg.2019.103445
17. S.H. Shelke, P.C. Mhaske, S.K. Kasam, V.D. Bobade, J. Heterocycl. Chem. **51**(6), 1893–1897 (2014). https://doi.org/10.1002/jhet.1910
18. Z. Shi, Z. Zhao, M. Huang, X. Fu, C. R. Chim. **18**(12), 1320–1327 (2015). https://doi.org/10.1016/j.crci.2015.09.005
19. S.H. Shelke, P.C. Mhaske, S. Narkhade, V.D. Bobade, J. Heterocycl. Chem. **51**(4), 1151–1156 (2014). https://doi.org/10.1002/jhet.1789

20. R. Listro, S. Stotani, G. Rossino, M. Rui, A. Malacrida, G. Cavaletti, M. Cortesi, C. Arienti, A. Tesei, D. Rossi, M.D. Giacomo, M. Miloso, S. Collina, Front. Chem. **8**, 495–495 (2020). https://doi.org/10.3389/fchem.2020.00495
21. G.D. Hatnapure, A.P. Keche, A.H. Rodge, S.S. Birajdar, R.H. Tale, V.M. Kamble, Bioorg. Med. Chem. Lett. **22**(20), 6385–6390 (2012). https://doi.org/10.1016/j.bmcl.2012.08.071
22. B. Selvakumar, N. Gujjar, M. Subbiah, K.P. Elango, Med. Chem. Res. **27**(2), 512–519 (2018). https://doi.org/10.1007/s00044-017-2077-5
23. J.A. Wiles, B.J. Bradbury, M.J. Pucci, Expert Opin. Ther. Pat. **20**(10), 1295–1319 (2010). https://doi.org/10.1517/13543776.2010.505922
24. M. Baumann, I.R. Baxendale, Beilstein J. Org. Chem. **9**(1), 2265–2319 (2013). https://doi.org/10.3762/bjoc.9.265
25. S.J.Y. Macalino, V. Gosu, S. Hong, S. Choi, Arch. Pharm. Res. **38**(9), 1686–1701 (2015). https://doi.org/10.1007/s12272-015-0640-5
26. X. Meng, H.-X. Zhang, M. Mezei, M. Cui, Curr. Comput. Aided-Drug **7**(2), 146–157 (2011). https://doi.org/10.2174/157340911795677602
27. S. Başoğlu Özdemir, *J. Turkish Chem. Soc.*, **3**(3), 515–534 (2016). https://doi.org/10.18596/jotcsa.55734
28. M.Y. Mentese, H. Bayrak, Y. Uygun, A. Mermer, S. Ulker, S.A. Karaoglu, N. Demirbas, Eur. J. Med. Chem. **67**, 230–242 (2013). https://doi.org/10.1016/j.ejmech.2013.06.045
29. E. Rajanarendar, K. Thirupathaiah, S. Ramakrishna, D. Nagaraju, Chin. Chem. Lett. **26**(12), 1511–1513 (2015). https://doi.org/10.1016/j.cclet.2015.07.024
30. A. Balabani, D.J. Hadjipavlou-Litina, K.E. Litinas, M. Mainou, C.-C. Tsironi, A. Vronteli, Eur. J. Med. Chem. **46**(12), 5894–5901 (2011). https://doi.org/10.1016/j.ejmech.2011.09.053
31. H. Bayrak, A. Demirbas, N. Demirbas, S.A. Karaoglu, Eur. J. Med. Chem. **44**(11), 4362–4366 (2009). https://doi.org/10.1016/j.ejmech.2009.05.022
32. Z. Peng, G. Wang, Q.-H. Zeng, Y. Li, Y. Wu, H. Liu, J.J. Wang, Y. Zhao, Food Chem. **341**, 128265–128265 (2021). https://doi.org/10.1016/j.foodchem.2020.128265
33. B.D. Vanjare, P.G. Mahajan, N.C. Dige, H. Raza, M. Hassan, Y. Han, S.J. Kim, S.-Y. Seo, K.H. Lee, Mol. Divers. (2020). https://doi.org/10.1007/s11030-020-10102-5
34. U. Cakmak, F. Oz-Tuncay, S. Basoglu-Ozdemir, E. Ayazoglu-Demir, İ Demir, A. Colak, S. Celik-Uzuner, S.S. Erdem, N. Yildirim, Med. Chem. Res. **30**(10), 1886–1904 (2021). https://doi.org/10.1007/s00044-021-02785-8
35. C.A. Lipinski, F. Lombardo, B.W. Dominy, P.J. Feeney, Adv. Drug Del. Rev. **23**(1–3), 3–25 (1997). https://doi.org/10.1016/S0169-409X(96)00423-1
36. D.F. Veber, S.R. Johnson, H.-Y. Cheng, B.R. Smith, K.W. Ward, K.D. Kopple, J. Med. Chem. **45**(12), 2615–2623 (2002). https://doi.org/10.1021/jm020017n
37. W. T. Ismaya, H. t. J. Rozeboom, A. Weijn, J. J. Mes, F. Fusetti, H. J. Wichers, B. W. Dijkstra, *Biochemistry*, **50**(24), 5477–5486 (2011). https://doi.org/10.1021/bi200395t
38. S. Jolivet, N. Arpin, H.J. Wichers, G. Pellon, Mycol. Res. **102**(12), 1459–1483 (1998). https://doi.org/10.1017/S0953756298006248
39. L. Gou, Z.-R. Lü, D. Park, S.H. Oh, L. Shi, S.J. Park, J. Bhak, Y.-D. Park, Z.-L. Ren, F. Zou, J. Biomol. Struct. Dyn. **26**(3), 395–401 (2008). https://doi.org/10.1080/07391102.2008.10507254
40. J.C. Espin, M. Morales, R. Varon, J. Tudela, F. Garciacanovas, Anal. Biochem. **231**(1), 237–246 (1995). https://doi.org/10.1006/abio.1995.1526
41. Y. Ozdemir, O. Bekircan, A. Colak, C. Dokuzparmak, *Indian J. Chem.*, **59**, 1409–1417 (2020). http://nopr.niscair.res.in/handle/123456789/55444
42. Y. Kolcuoğlu, A. Colak, E. Sesli, M. Yildirim, N. Saglam, Food Chem. **101**(2), 778–785 (2007). https://doi.org/10.1016/j.foodchem.2006.02.035
43. C. Molinspiration (2016). http://www.molinspiration.com/cgi-bin/properties
44. Y.H. Zhao, M.H. Abraham, J. Le, A. Hersey, C.N. Luscombe, G. Beck, B. Sherborne, I. Cooper, Pharm. Res. **19**(10), 1446–1457 (2002). https://doi.org/10.1023/A:1020444330011
45. S. Wavefunction (2016). http://wavefun.com
46. J.J.P. Stewart, J. Mol. Model. **15**(7), 765–805 (2009). https://doi.org/10.1007/s00894-008-0420-y
47. Y. Zhao, D.G. Truhlar, Acc. Chem. Res. **41**(2), 157–167 (2008). https://doi.org/10.1021/ar700111a
48. Y. Zhao, D.G. Truhlar, Theor. Chem. Acc. **120**(1–3), 215–241 (2008). https://doi.org/10.1007/s00214-007-0310-x
49. O. Trott, A.J. Olson, J. Comput. Chem. **31**(2), 455–461 (2009). https://doi.org/10.1002/jcc.21334
50. G.M. Morris, R. Huey, W. Lindstrom, M.F. Sanner, R.K. Belew, D.S. Goodsell, A.J. Olson, J. Comput. Chem. **30**(16), 2785–2791 (2009). https://doi.org/10.1002/jcc.21256
51. Accelrys Software Inc. Release 4.0, San Diego, Discovery Studio Modeling Environment (2013).